A TIME-RESOLVED HIGH CHARGE DENSITY ELECTRON PHOTOEMISSION MODEL FOR THE FCC-ee TOP-UP SCHEME

A. Omoumi*, E. Granados, A. Latina, M. Martinez-Calderon
European Organization for Nuclear Research [CERN], Geneva, Switzerland
L. Jones, Science and Technology Facilities Council, Swindon, United Kingdom

Abstract

The generation of ultrabright electron beams relies on photo-injectors, which are influenced by dynamic surface and collective field effects. Predicting the resulting bunch characteristics is complicated due to the superposition of RF field, near cathode image-charge field, and space-charge. These effects are particularly relevant in high charge density photo-injectors operating with sub-ps bunch duration and nC bunch charge. We present an extended Fowler–Dubridge–canonical photoemission model that incorporates self-consistenly the temporal evolution of the aforementioned surface electric fields. We perform this connection by dynamically coupling the resulting fiends and the Schottky barrier. This method links single-particle photoemission physics with collective field effects, enabling the prediction of quantum yield in real time. Our simulations reveal strong spatio-temporal modulation of the photoemissive process, inducing nonlinear collective forces that degrade beam quality through emittance growth and phase-space distortion. The results underscore the important role in shaping the initial laser pulses to tailor the phase space of electron bunches for future colliders.

INTRODUCTION

Top-up injection is a key requirement for FCC-ee to sustain high integrated luminosity and ultimately sets the performance envelope of the machine. For instance, in the $t\bar{t}$ mode at 175 GeV, the nominal beam lifetime of 1 h is already the shortest among the four planned operating points, and in practice is likely to be even lower. Therefore a robust and reliable top-up injection scheme is therefore essential [1].

A first design of the FCC-ee electron gun has been proposed and optimized to meet the specifications of the accelerator complex [2]. The target energy of 200 MeV is achievable while keeping the rms transverse emittance below 4 mm·mrad and the rms bunch length near 1 mm at a peak charge of 5 nC. The high-charge density and ultrafast nature of these bunches induce collective charge fields can reshape the surface potential on femtosecond timescales. The emitted electrons generate a rapidly varying collective field that raise the effective photocathode potential barrier and can partially suppress the photoemission process half way through the laser pulse, distorting the emerging electron bunch phase space [3, 4]. These effects cannot be described in the traditional canonical or analytical simulation frameworks where photoemission is treated as an instantaneous process under quasi-static applied fields.

Particle-in-Cell (PIC) and point-to-point Coulomb solvers treat fields and particle motion self-consistently, accounting for shielding, bunch loading, and geometric field curvature [5–7]. While accurate at the device scale, they require external emission laws, cannot resolve ångström-scale barrier dynamics at practical mesh sizes, and are too computationally intensive for real-time injector optimisation or feedback loops needed in a top-up regime [1, 2].

Canonical photoemission models, including Fowler–DuBridge photoemission, thermal emission, and field emission formulations, provide fast local estimates of current density and incorporate microscopic barrier physics such as Schottky lowering and image potential [8–10]. However, they assume static applied fields and therefore cannot capture the transient collective-field modulation that occurs during high-brightness ultrafast emission.

These limitations motivate the development of a self consistent emission model that bridges microscopic barrier physics with macroscopic collective-field evolution. The model presented here incorporates dynamic modulation of the barrier potential [11, 12]. Its low computational cost makes it suitable for real-time on-demand charge control, aligning directly with the operational requirements of FCC-ee top-up injection scheme.

TIME-RESOLVED PHOTOEMISSION MODEL

A predictive description of photoemission in RF injectors must link microscopic barrier physics with the macroscopic collective fields that evolve during emission. The interplay of the optical laser pulse, photocathode properties, and near-surface charge buildup sets the emission rate (or dynamic quantum yield) and initial phase space, and thus the beam brightness. We introduce here a time-dependent Fowler–DuBridge model that includes dynamic Schottky lowering and self-consistent image- and space-charge feedback.

Because photoemission is confined to the laser spot footprint on the photocathode surface, the emerging charge distribution can be treated as a finite disk rather than the idealized infinite sheet often used in analytic injector models [13]. The infinite-sheet approximation overestimates near-surface screening and artificially clamps the emission current [3, 14, 15].

* anahita.omoumi@cern.ch

We represent the bunch as a sequence of thin, expanding charge disks of instantaneous radius $a_j(t)$ and surface density $\sigma_j(t) = q_j/(\pi a_j^2)$. The on-axis longitudinal field produced by a uniformly charged disk of radius a at a distance Δz above the disk is

$$E_{\text{disk}}(\Delta z; a) = \frac{\sigma}{2\varepsilon_0}\left(1 - \frac{\Delta z}{\sqrt{\Delta z^2 + a^2}}\right). \tag{1}$$

This closed-form kernel is used for both the image-charge field at the cathode surface and the vacuum space-charge field acting on electrons after emission.

During emission, the total field near the photocathode consists of the applied RF field (F_{RF}) and the collective fields generated by the emerging bunch [10]. To treat emission and transport consistently, we separate the surface (barrier) field from the field acting on electrons once they leave the photocathode. The barrier field governing Fowler-DuBridge emission is

$$F_{\text{bar}}(t) = F_{\text{RF}} - E_{\text{IC}}(t), \tag{2}$$

where $E_{\text{IC}}(t)$ is the image-charge field evaluated at the surface using the finite-disk kernel. This field modulates the instantaneous Schottky lowering and thus the emission current. The field acting on electrons in vacuum is

$$F_{\text{dyn}}(t, z_i) = F_{\text{RF}} - E_{\text{SC}}(t, z_i), \tag{3}$$

where $E_{\text{SC}}(t, z_i)$ is the vacuum space-charge field produced by all previously emitted disks located closer to the cathode. This decomposition avoids double counting: the image field influences only the emission barrier, while the vacuum space-charge field governs the longitudinal dynamics after emission. Together with the finite-disk representation, this provides a consistent time-dependent surface field for the Fowler–DuBridge emission model.

This configuration is illustrated in Fig. 1. The cathode at $z = 0$ emits thin, expanding charge disks that experience the transport field $F_{\text{dyn}}(t, z_i)$ in vacuum, while the emission barrier is set by the surface field $F_{\text{bar}}(t)$. The diagram highlights how the image field acts only at the surface, whereas the vacuum space-charge field governs the longitudinal dynamics after emission.

For calculating the image-charge field at the surface, we treat it as if each emitted disk produces an image disk of opposite charge inside the cathode. Evaluated at the surface ($z = 0^+$), the total image field is then

$$E_{\text{IC}}(t) = \frac{1}{\varepsilon_0 A}\sum_{j\in P(t)} q_j\left(1 - \frac{z_j}{\sqrt{z_j^2 + a_j^2}}\right)\exp\left[-\frac{z_j}{Z_{\text{mat}}}\right], \tag{4}$$

where $A = \pi r_x r_y$ is the laser spot area, $z_j(t)$ and $a_j(t)$ are the height and radius of sheet j, and Z_{mat} represents the material's finite image-charge penetration depth. The exponential factor suppresses the image interaction once electrons move several microns from the cathode.

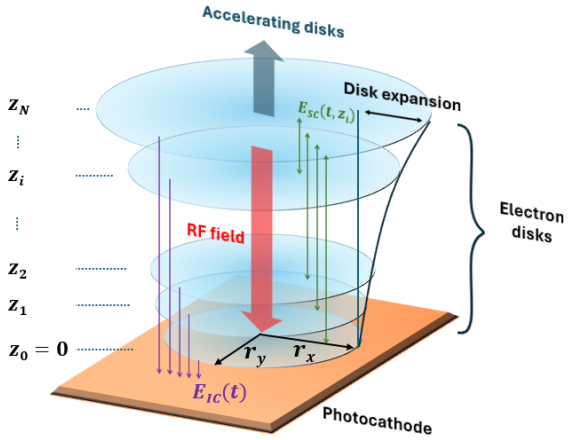

Figure 1: Field decomposition during photoemission. The surface field $F_{\text{bar}}(t)$ includes the image-charge contribution, while electrons in vacuum evolve under the transport field $F_{\text{dyn}}(t, z_i)$. The schematic separates surface barrier effects from space-charge forces after emission.

Beyond the near-surface region, electrons interact through the vacuum space-charge field. For a sheet at position $z_i(t)$, the space-charge field generated by all the other electron sheets j is

$$E_{\text{SC}}(t, z_i) = \sum_{j: z_j < z_i} \frac{q_j}{\pi a_j^2}\frac{1}{2\varepsilon_0}\left(1 - \frac{z_i - z_j}{\sqrt{(z_i - z_j)^2 + a_j^2}}\right). \tag{5}$$

Each disk expands radially due to the intrinsic thermal momentum spread and space charge forces. Using a ballistic approximation, the radius evolves as

$$a_j(t) = \sqrt{a_0^2 + (v_r t)^2}, \qquad v_r = \sqrt{\frac{2\,\text{MTE}}{m_e}}, \tag{6}$$

where MTE is the mean transverse energy and a_0 is the initial laser spot radius.

The dynamic net surface electric field obtained from the finite-disk image-charge model is coupled to a time-dependent Fowler-DuBridge (FD) emission model. The instantaneous barrier field $F_{\text{bar}}(t)$ determines the Schottky reduction of the work function as

$$\Delta\phi_{\text{S}}(t) = \sqrt{\frac{e^3 F_{\text{bar}}(t)}{4\pi\varepsilon_0}}, \qquad \phi_{\text{eff}}(t) = \phi - \Delta\phi_{\text{S}}(t), \tag{7}$$

so that the FD photoemission supply becomes

$$J_{\text{FD}}(t) = A_{\text{FD}}\,[h\nu - \phi_{\text{eff}}(t)]^2 \exp\left[-\frac{B}{F_{\text{bar}}(t)}\right] I(t), \tag{8}$$

where A_{FD} is a material constant and $I(t)$ is the laser temporal profile. This formulation captures how the buildup of collective image charge increases $F_{\text{bar}}(t)$ and suppresses emission mid-pulse. When the photon energy falls below

the instantaneous emission threshold, a tunneling factor is applied using the RF-tilted, image-corrected barrier,

$$V(z,t) = \phi - eF_{\mathrm{bar}}(t)z - \frac{e^2}{16\pi\varepsilon_0 z}, \tag{9}$$

with transmission coefficient

$$T(t) = \exp\left[-\frac{2}{\hbar}\int_{z_1}^{z_2}\sqrt{2m_e V(z,t)}\,dz\right], \tag{10}$$

so that the emitted current density is

$$J(t) = J_{\mathrm{FD}}(t)\,T(t). \tag{11}$$

Because $F_{\mathrm{bar}}(t)$ already includes the finite-disk image field with material attenuation, this closure links microscopic barrier physics to the macroscopic charge evolution. As emission proceeds, early electrons enhance the near-surface field, increasing the Schottky barrier for later electrons and producing the self-modulated emission profiles characteristic of ultrafast, high-charge operation.

EXPERIMENTAL VALIDATION

To validate the time-dependent emission model, we compare its predictions with measurements performed in a 1.6-cell S-band RF gun operating at ~120 MV/m with a copper photocathode under a range of UV illumination conditions, constructed for the AWAKE run2c experiment [16, 17]. The UV pulses at 257 nm, derived from a frequency-quadrupled Yb:KGW system, delivered a few to tens of microjoules to the cathode with adjustable spot size and pulse duration [18]. The beamline includes a solenoid for emittance compensation and diagnostics consisting of a YAG:Ce screen, a dipole spectrometer, and a Faraday cup. Shot-to-shot laser profiles and energies were monitored and used as inputs to the model. Electron bunches of typically a few hundred pC were generated and accelerated to ~6 MeV at 0.8–10 Hz repetition rate.

Figure 2 compares the simulated and measured bunch charge as a function of UV pulse energy for several pulse durations. The model reproduces the observed sublinear scaling and the onset of saturation at high laser pulse fluence. Short pulses (265 fs) generate higher peak emission rates and therefore reach charge clamping earlier, whereas longer pulses produce weaker instantaneous space-charge fields and maintain a nearly linear charge-UV pulse energy relation. The corresponding simulated quantum-efficiency curves follow closely the experimental trend, indicating that the collective-field coupling is precisely captured.

The simulations also provide the transient barrier field and emission current. For the 265 fs pulse, the high peak fluence causes the image field to rise rapidly to almost 20 MV/m, suppressing mid-pulse emission and producing an asymmetric current profile that saturates around 700 - 800 pC. For the 1.5 ps pulse, the slower laser envelope limits the image-field growth to approximately 8–10 MV/m near the pulse peak, allowing emission to follow the laser shape more closely and giving an almost linear charge scaling up to ≈ 250 pC.

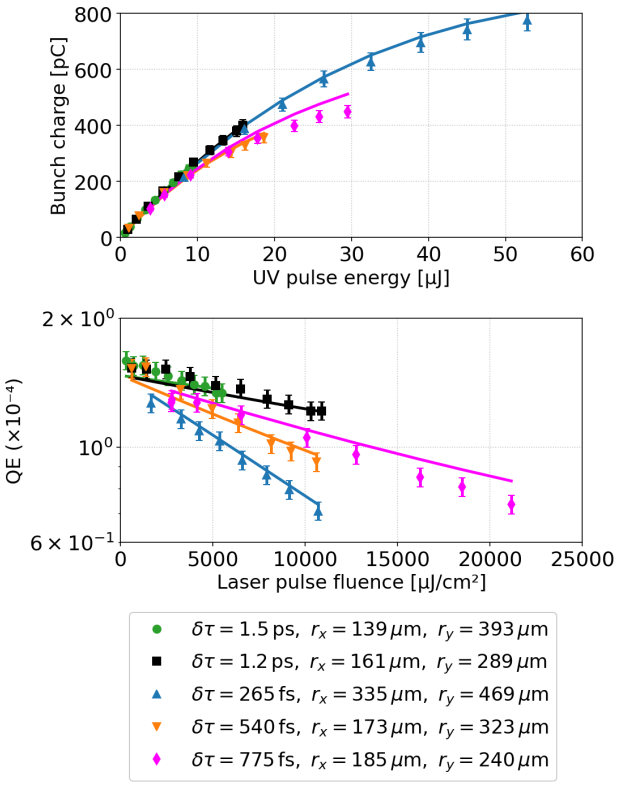

Figure 2: Simulated (solid lines) and experimental (markers) of bunch charge vs. UV pulse energy (top) and quantum yield vs. fluence for deep-UV pulses (bottom) with different illumination parameters at the photocathode surface.

CONCLUSION AND OUTLOOK

The model presented here provides a fast, self-consistent description of ultrafast photoemission, capturing the transient evolution of the surface barrier and the collective image- and space-charge fields. By resolving these dynamics in time, the simulations reproduce the measured charge saturation and fluence dependence over a wide operating range, while also predicting the emission asymmetry [19, 20]. This confirms that the approach captures both microscopic barrier physics and macroscopic collective effects with low computational cost.

Looking ahead, this framework will be extended toward adaptive control of the UV pulse to enable real-time charge tuning in the FCC-ee injector. Such capability is a key requirement for stable top-up operation, where precise bunch-charge regulation must be maintained despite varying laser and machine conditions [1, 2, 21]. Integrating this model into the source design workflow will support the development of high-brightness injectors tailored to the demands of future collider facilities.

REFERENCES

[1] M. Aiba *et al.*, "Top-up injection schemes for future circular lepton collider", *Nucl. Instrum. Methods Phys. Res. A*, vol. 880, pp. 98–106, 2018.

doi:10.1016/j.nima.2017.10.075

[2] Z. Vostrel and S. Doebert, "Design of an electron source for the FCC-ee with top-up injection capability", *Nucl. Instrum. Methods Phys. Res. A*, vol. 1063, p. 169261, 2024. doi:10.1016/j.nima.2024.169261

[3] Z. Tao, H. Zhang, P. M. Duxbury, M. Berz, and C.-Y. Ruan, "Space charge effects in ultrafast electron diffraction and imaging", *J. Appl. Phys.*, vol. 111, p. 044316, 2012. doi:10.1063/1.3685747

[4] K. L. Jensen *et al.*, "Modeling emission lag after photoexcitation", *J. Appl. Phys.*, vol. 122, p. 164501, 2017. doi:10.1063/1.5008366

[5] M. Gordon, S. B. van der Geer, J. Maxson, and Y.-K. Kim, "Point-to-point Coulomb effects in high brightness photoelectron beam lines for ultrafast electron diffraction", *Phys. Rev. Accel. Beams*, vol. 24, p. 084202, 2021. doi:10.1103/PhysRevAccelBeams.24.084202

[6] R. A. Kishek *et al.*, "Simulations and experiments with space-charge-dominated beams", *Phys. Plasmas*, vol. 10, pp. 2016–2021, 2003. doi:10.1063/1.1558291

[7] Y. Chen *et al.*, "Modeling and simulation of RF photoinjectors for coherent light sources", *Nucl. Instrum. Methods Phys. Res. A*, vol. 889, pp. 129–137, 2018. doi:10.1016/j.nima.2018.02.017

[8] Y. Zhou and P. Zhang, "A quantum model for photoemission from metal surfaces and its comparison with the three-step model and Fowler–DuBridge model", *J. Appl. Phys.*, vol. 127, p. 164903, 2020. doi:10.1063/5.0004140

[9] K. L. Jensen, *Introduction to the Physics of Electron Emission*, Hoboken, NJ, USA: Wiley, 2017. doi:10.1002/9781119051794

[10] D. H. Dowell and J. F. Schmerge, "Quantum efficiency and thermal emittance of metal photocathodes", *Phys. Rev. ST Accel. Beams*, vol. 12, p. 074201, 2009. doi:10.1103/PhysRevSTAB.12.074201

[11] K. L. Jensen, "A thermal-field-photoemission model and its application", in *Modern Developments in Vacuum Electron Sources*, Springer, Cham, 2020, pp. 345–385. doi:10.1007/978-3-030-47291-7_8

[12] J. Portman *et al.*, "Untangling the contributions of image charge and laser profile for optimal photoemission of high-brightness electron beams", *J. Appl. Phys.*, vol. 116, p. 173105, 2014. doi:10.1063/1.4900582

[13] M. Reiser, *Theory and Design of Charged Particle Beams*, 2nd ed. Weinheim, Germany: Wiley-VCH, 2008. doi:10.1002/9783527622047

[14] A. Valfells *et al.*, "Effects of pulse-length and emitter area on virtual cathode formation in electron guns", *Phys. Plasmas*, vol. 9, pp. 2377–2382, 2002. doi:10.1063/1.1463065

[15] S. B. van der Geer, M. J. de Loos, and O. J. Luiten, "Pancakes versus beer-cans in terms of 6D phase-space density", in *Proc. EPAC'08*, Genoa, Italy, 2008, p. 151.

[16] E. Gschwendtner *et al.*, "The AWAKE Run 2 programme and beyond", *Symmetry*, vol. 14, p. 1680, 2022. doi:10.3390/sym14081680

[17] V. Musat *et al.*, "Status of the commissioning of the X-band injector prototype for AWAKE Run 2c", in *Proc. IPAC'24*, Nashville, USA, 2024, paper MOPC28. doi:10.18429/JACoW-IPAC2024-MOPC28

[18] E. Granados *et al.*, "Optical and laser systems for the AWAKE Run 2C experiment", in *Proc. IPAC'25*, Geneva, Switzerland, 2025, pp. 1604–1607. doi:10.18429/JACoW-IPAC2025-TUPS111

[19] L. Serafini and J. B. Rosenzweig, "Envelope analysis of intense relativistic quasilaminar beams in RF photoinjectors", *Phys. Rev. E*, vol. 55, pp. 7565–7577, 1997. doi:10.1103/PhysRevE.55.7565

[20] P. Musumeci *et al.*, "Experimental generation and characterization of uniformly filled ellipsoidal electron-beam distributions", *Phys. Rev. Lett.*, vol. 100, p. 244801, 2008. doi:10.1103/PhysRevLett.100.244801

[21] A. Abada *et al.*, "FCC-ee: The lepton collider: Future circular collider conceptual design report, volume 2", *Eur. Phys. J. Spec. Top.*, vol. 228, no. 2, pp. 261–623, 2019. doi:10.1140/epjst/e2019-900045-4